

See discussions, stats, and author profiles for this publication at: <https://www.researchgate.net/publication/258458516>

Geochemical investigations of saltwater intrusion into the coastal carbonate aquifer of Mallorca, Spain

Article in *Applied Geochemistry* · December 2013

DOI: 10.1016/j.apgeochem.2013.09.011

CITATIONS

17

READS

514

4 authors, including:



Charlotte Garing
University of Georgia

17 PUBLICATIONS 121 CITATIONS

[SEE PROFILE](#)



Linda Luquot
Spanish National Research Council

79 PUBLICATIONS 1,269 CITATIONS

[SEE PROFILE](#)



Philippe Adrien Pezard
French National Centre for Scientific Research

190 PUBLICATIONS 2,384 CITATIONS

[SEE PROFILE](#)

Some of the authors of this publication are also working on these related projects:



Deep drilling of ocean basement 1: DSDP/ODP Hole 504B (equatorial Pacific Ocean) [View project](#)



CO2 sequestration [View project](#)



Geochemical investigations of saltwater intrusion into the coastal carbonate aquifer of Mallorca, Spain



C. Garing^{a,*}, L. Luquot^{a,b}, P.A. Pezard^a, P. Gouze^a

^a Géosciences Montpellier, UMR 5243 CNRS/INSU, CC60, Université de Montpellier 2, Pl. E. Bataillon, 34095 Montpellier cedex 5, France

^b Institute of Environmental Assessment and Water Research (IDAEA), Pascual Vila Building, Office 625, C/Jordi Girona 18, 08034 Barcelona, Spain

ARTICLE INFO

Article history:

Received 27 September 2012

Accepted 24 September 2013

Available online 30 September 2013

Editorial handling by A. Vengosh

ABSTRACT

Coastal aquifers often display seawater intrusion resulting in the formation of a salty water wedge progressing inland. This study investigates the mass transfers in the mixing zone at the freshwater–seawater interface where the water is out of equilibrium with the rock-forming carbonates. Investigations were conducted in two boreholes, separated by 5 m, at the Ses Sitjoles test site (Mallorca Island, Spain) where repeated electrical conductivity logs of the formation and the saturating fluid, as well as regular pore-water sampling and permanent downhole multi-parameter monitoring of the water were performed over a period of 9 a. In the mixing zone, the significant acidification, the calcite saturation index profile and the Ca concentration profile cannot be explained by conservative mixing nor by dissolution–precipitation reactions only. Conversely, the analysis of organic C content and of the distinctly different time-resolved pH profiles measured in the two boreholes suggests the development of perennial biomass that triggers calcite dissolution. Moreover, the presence of biomass seems to be correlated with the permeability and vertical connectivity at the meter-scale. It is speculated that the mechanism could be self-activated because the microbiological activity induces calcite dissolution and tends to increase porosity and permeability that favors biomass development.

© 2013 Elsevier Ltd. All rights reserved.

1. Introduction

Many coastal aquifer reservoirs are subjected to severe saltwater intrusion, particularly in Mediterranean regions where massive withdrawals of freshwater for touristic or agricultural purposes occur during the driest period (Bear et al., 1999; Llamas and Custodio, 2003; Arfib and de Marsily, 2004; Pulido-Leboeuf, 2004). The freshwater–saltwater mixing zone, resulting from density-driven flow and hydrodynamic dispersion and diffusion (Ghyben, 1889; Herzberg, 1901; Cooper, 1964; Henry, 1964; Abarca et al., 2007), has frequently been demonstrated to be the locus of complex geochemical processes: the identified processes that may affect the groundwater geochemistry are (i) the mixing of the groundwater and the intruded seawater, (ii) carbonate dissolution/precipitation, (iii) ion exchange and silicate (largely clay) diagenesis and (iv) redox reactions (Appelo and Postma, 1993; Jones et al., 1999; Vengosh, 2003).

The water–rock interactions in the mixing zone in coastal carbonate aquifers have been of considerable interest because of the possible effect of seawater intrusion altering the groundwater flow system. The mixing of freshwater and saltwater, even with both at equilibrium with carbonate minerals, results in an undersaturated

solution (Runnels, 1969; Plummer, 1975; Wigley and Plummer, 1976), which then has the potential to dissolve the carbonate formations. Calcite undersaturation and calcite dissolution have been proved to occur in a freshwater–seawater mixing zone (Hanshaw and Back, 1980; Smart et al., 1988; Stoessel et al., 1989; Whitaker and Smart, 1997; Baceta et al., 2001). However, no subsaturation or dissolution evidence has been found in some other cases (Maliva et al., 2001; Melim et al., 2002) and even supersaturated waters with respect to calcite have been found in a mixing zone (Price and Herman, 1991; Ng and Jones, 1995; Wicks and Herman, 1996). Also, while some studies report evidence of active dolomitization processes in a current mixing zone (Gonzales and Ruiz, 1991; Pulido-Leboeuf, 2004), others report no signs of dolomite formation although the waters are supersaturated with respect to dolomite (Smart et al., 1988; Stoessel et al., 1989; Maliva et al., 2001; Melim et al., 2002).

In order to properly understand the interplay between transport and chemistry in mixing zones, Sandford and Konikow (1989a,b) proposed a fully coupled reactive transport model and showed that significant carbonate dissolution may occur due to the mixing of freshwater and saltwater. Rezaei et al. (2005) reported similar results using a more sophisticated modeling approach. An alternative model was proposed by Romanov and Dreybrodt (2006). Their results were in good agreement with field observations and laboratory dissolution experiments (Singurindy

* Corresponding author. Tel.: +33 467143664; fax: +33 467143244.

E-mail address: charlotte.garing@gm.univ-montp2.fr (C. Garing).

et al., 2004) of carbonate reactions in synthetic mixtures of saturated waters. Singurindy et al. (2004) observed calcite dissolution; however, the experimental design did not allow quantitative study of the relationship between the subsaturation of the injected fluid and the observed dissolution. Sanz et al. (2011) conducted flow-through experiments on calcite dissolution by mixing waters and found high sensitivity of the amount of calcite dissolved to mixing ratio and minor variations of PCO_2 .

All of these previous studies highlight the complexity of geochemical processes associated with a mixing zone and especially the difficulty of anticipating whether or not dissolution will occur, and where exactly it might be located within the intruded coastal aquifer. In order to further investigate the impact of a mixing zone on the porosity evolution of coastal reservoirs, long-term field studies coupling *in situ* geochemical analysis and investigation of reservoir rock properties are needed.

The aim of this paper is two-fold. First the current saltwater intrusion at the Ses Sitjoles site (Spain) and its evolution with time are characterized using a set of borehole data recorded over 8 a (conductivity profiles, groundwater sampling and permanent downhole multi-parameter monitoring). Second the biogeochemical processes likely to occur within the mixing zone and thus modify the structure and the hydraulic properties of the reservoir are investigated by a coupled analysis of the groundwater composition and the reservoir properties.

2. Materials and methods

2.1. Mallorca experimental site

The experimental site, named the Ses Sitjoles site, in the SE of Mallorca island, 6 km away from the coast, near the city of Campos (Fig. 1), has been equipped since 2003. The site comprises 18 boreholes drilled or cored to 100 m depth in an area of 114 m × 87 m. These boreholes sample the Lluçmajor carbonate platform: a Miocene reef body characterized by internal platform-like structures at the top, karstified reef-like constructions in the middle and forereef deposits at the base. Spectacular outcrops of the prograding Miocene reef complex are found along nearby high sea-cliffs. The large scale structure of this reef body has been extensively described (Esteban, 1979; Pomar et al., 1996; Pomar and Ward, 1999). A large number of data have been collected since 2003 at the Ses Sitjoles site, allowing a good description of the structural, petrophysical and geochemical variability, and heterogeneity of the reservoir (Jaeggi, 2006; Maria-Sube, 2008; Hebert, 2011; Garing, 2011).

The main geological and petrophysical features established in the studies listed above are summarized for a vertical open borehole called MC2, which is the reference cored hole at the Ses Sitjoles site. The barrier reef unit, from 25 to 61.7 m below the surface (mbs) is in a coral-rich zone with skeletal packstones, coral and algae floatstones and framestones, and many bioclasts. Dolomite is found at 34, 48 and from 59 to 61.7 mbs. The variability of the facies and the diagenetic events of dissolution and cementation result in a heterogeneous porosity with highly indurated low porous zones (around 37, 48 and from 56 to 61.7 mbs) separated by dissolution cavities of a few meters and moldic pores of a few centimeters. The forereef unit (from 61.7 to 100 mbs) consists of micritic skeletal packstones with an important moldic microporosity and some algae or peloid fragments and a few other bioclasts, with a major dolomitized level from 84 to 89 mbs. The overall forereef unit is much more homogeneous than the barrier reef unit. The porosity is mostly intergranular and moldic (from dissolved bioclasts) with values around 0.40 (Hebert, 2011). The studied part of the aquifer, which is the saturated part from 40 to 100 mbs, does not contain any clay material, even in small amounts, and in the following, ion-exchange reactions were considered to be minor compared with carbonate dissolution-precipitation processes. A main feature of the Lluçmajor aquifer is the presence of massive sea water intrusion that has progressively spread inland during the past 30 a (1980–2010) and now has intruded more than 10 km from the shore (Fig. 1). At the experimental site of Ses Sitjoles, the water table is located around 38 mbs and the freshwater becomes brackish around 60 mbs.

Mallorca Island has a typical Mediterranean climate, characterized by mild winters and hot dry summers. Most of the precipitation occurs during September and October, which represents more than 50% of the annual rainfall, and it almost never rains during June, July and August. From 2001 to 2011 the rain gauge station of Lluçmajor Mas Deu, located near the studied site, recorded an average annual rainfall of 490 mm, with variation from one year to another (289 mm in 2005 and 725 mm in 2007 for example). The maximum temperatures in the SE part of the Island occur in July–August, with a mean monthly temperature of 25 °C, and they reach minimum values in December–January, with a mean monthly temperature of 8.5 °C (Kent et al., 2002). The high consumption of freshwater for touristic and agricultural purposes which regularly exceeds the natural recharge of the aquifer and increases during the driest period, is responsible for the contamination of the reservoir by the seawater intrusion (Deya Tortella and Tirado, 2011).

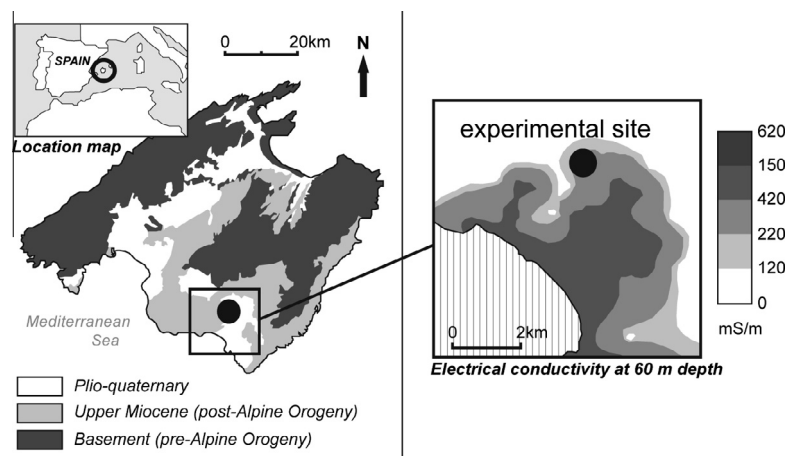


Fig. 1. Simplified geological map of Mallorca with the experimental site location (left) and electrical conductivity map at 60 m depth highlighting an on-going saltwater intrusion in that particular zone (right, data from the Environmental Ministry of the Government of the Balearic Islands).

2.2. Geophysical and petrophysical analysis

An extensive set of borehole geophysical data have been collected at this site since its creation in 2003. For the present study, the focus is on boreholes MC2 and MC8.

Two parameters have received special attention when it comes to studying the location and evolution of the saltwater intrusion: the electrical conductivity of the formation (water-saturated rock) and the electrical conductivity of the pore-water. The conductivity of the saturated reservoir rock (σ_r) was obtained from deep resistivity and medium induction resistivity profiles ($\rho_r = 1/\sigma_r$) recorded using the dual focused resistivity probe DLL5 from GeoVista and the Dual Induction Laterolog DIL45 from ALT (Advanced Logic Technology), respectively, with a precision of 0.05 mS/cm in each case. The DLL is more accurate in freshwater-saturated formations whereas the DIL is preferred in saline water environments (Schlumberger, 1972, 1974). The electrical conductivity of the pore-water, σ_f , was measured in the open borehole using an Ocean Seven 302 CTD probe from IDRONAUT with an error of 0.04 mS/cm. This multi-parameter tool also provides measurements of pH, with an error of 0.05 pH. The profiles of the formation and fluid electrical conductivity were recorded in MC2 and MC8 from 40 to 95 mbs, which corresponds to the saturated part of the reservoir. In addition, two permanent sensors Greenspan (HYDREKA) recording the electrical conductivity of the water every hour (error of 1% + 0.05 mS/cm) were installed in borehole MC8 in February 2008, at 60 and 70 mbs.

The rock structure was investigated using borehole images recorded with the optical televiewer OBI40 from ALT. In addition to the borehole images, the microstructures were investigated using thin section observations with an optical microscope.

Porosity and permeability were measured on 21 cylindrical plugs of 40 mm diameter and 60 mm length regularly sampled in MC2 borehole core from 40 to 100 m depth by conducting the He injection method (Klinkenberg, 1941). The permeability was corrected from the Klinkenberg effect under stress (Jones, 1972).

2.3. Water sampling and chemical analysis

Groundwater samples were collected from 40 to 95 mbs in May 2005, February 2008 and July 2011. For each sampling campaign, Table 1 summarizes the boreholes and depths where the water was sampled, the sampling system which was used, the chemical elements which were analyzed and analytical method, and also which corresponding *in situ* pH data are available (“downhole pH profiles” refers to the pH measured in the boreholes with the IDRONAUT tool). All the major element concentrations were determined with a detection limit of 0.05 $\mu\text{g/L}$ and are given with an error of 3%. In all cases the alkalinity, expressed in concentration of HCO_3^- , was measured in the laboratory by HCl titration and Gran plot with a precision of 0.2%. Before 2010, a stainless steel bailer with solenoid valves that are electrically activated from the surface was used to sample the groundwater inside the borehole. In summer 2010 a multilevel groundwater monitoring system Westbay

(WB) from Schlumberger Water Services (Black et al., 1986) was placed in borehole MC2. This equipment allows *in situ* sampling of the pore fluid at the formation pressure. Furthermore, back on the surface, the sampling bottles, kept closed, were connected to a special device containing a pH sensor InPro 4800i (error between 0.03 and 0.05 pH and reproducibility between 0.01 and 0.02 pH) and a dissolved O_2 sensor InPro 6850i (error below 1% + 6 ppb) by Mettler Toledo, allowing the measurement of the *in situ* values of each parameter before the water equilibrates with the atmospheric pressure. Indeed when the bottle is opened at the surface, atmospheric CO_2 and O_2 equilibrate with the solution and, consequently, pH is modified. Total organic C (TOC) was also determined on the groundwater sampled in 2011, using a total organic C analyzer from Shimadzu (accuracy of 0.5%).

In addition to these groundwater samples, sea water samples were collected at two different locations near the site in July 2011 for comparison with the saltwater found at depth in the boreholes.

The saturation state of the waters with respect to calcite and dolomite and the CO_2 content (expressed as $\log(\text{pCO}_2)$ in the following) were calculated using the aqueous speciation model PHREEQC with the Pitzer ion–ion interaction coefficients (Parkhurst and Appelo, 1999), using the mean water composition, the HCO_3^- concentration, the pH and the temperature of the groundwater. The difference between data obtained using the Pitzer’s ion interaction model and data calculated using the specific-ion interaction model of PHREEQC is below 0.05 for the saturation index (for calcite and dolomite) and below 0.02 for $\log(\text{pCO}_2)$. The same geochemical model was also used to simulate the conservative mixing of the two end-member solutions (freshwater at 40 m depth and saltwater at 85 m depth) with different mixing ratios for comparison with the sampled waters, knowing that a deviation in the observed groundwater chemistry in the mixing zone from the mixing-generated values (that are later named ΔCa and ΔMg for Ca and Mg, respectively) can be considered as evidence of non-conservative processes occurring in the studied zone. The Cl^- concentration of the samples was used to calculate the fraction of saltwater, assuming that Cl^- is a conservative element in the mixing process and that the only source of Cl^- in the groundwater is saltwater.

3. Results

3.1. Geophysical characterization and monitoring of the saltwater intrusion

The profiles of the electrical conductivity of the formation and of the water characterizing the saltwater intrusion in boreholes MC2 and MC8 are presented in Fig. 2, together with pH profiles.

Fig. 2a displays the formation electrical conductivity logs recorded in boreholes MC2 and MC8 in October 2010 with the galvanic tool (measurement of deep resistivity logs: RLLD expressed as conductivity) and the induction tool (medium induction logs: ILM). For each borehole, the measurements recorded with both tools are similar. Since more data recorded with the induction tool

Table 1
Information concerning the groundwater samples (year, borehole, depths, sampling system, ion analysis, and available *in situ* pH data).

Year	Borehole	Depths (m)	Sampling system	Major elements analysis	pH
2005	MC2	70, 94	Bailer	Ca, Mg, Na, K, Cl, SO_4 , NO_3 (ion chromatography)	Downhole pH profiles
	MC8	40, 63, 72, 85			
2008	MC2	40, 58, 65, 70, 75, 85	Bailer	Ca, Mg, Na, K, Fe, Si (atomic emission spectroscopy) Cl (electrophoresis ion chromatography)	Downhole pH profiles
2011	MC2	40, 51, 64, 71, 77, 85	Westbay Sampler	Ca, Mg, Na, K (atomic emission spectroscopy) Cl, SO_4 (electrophoresis ion chromatography)	pH of the Sampled water

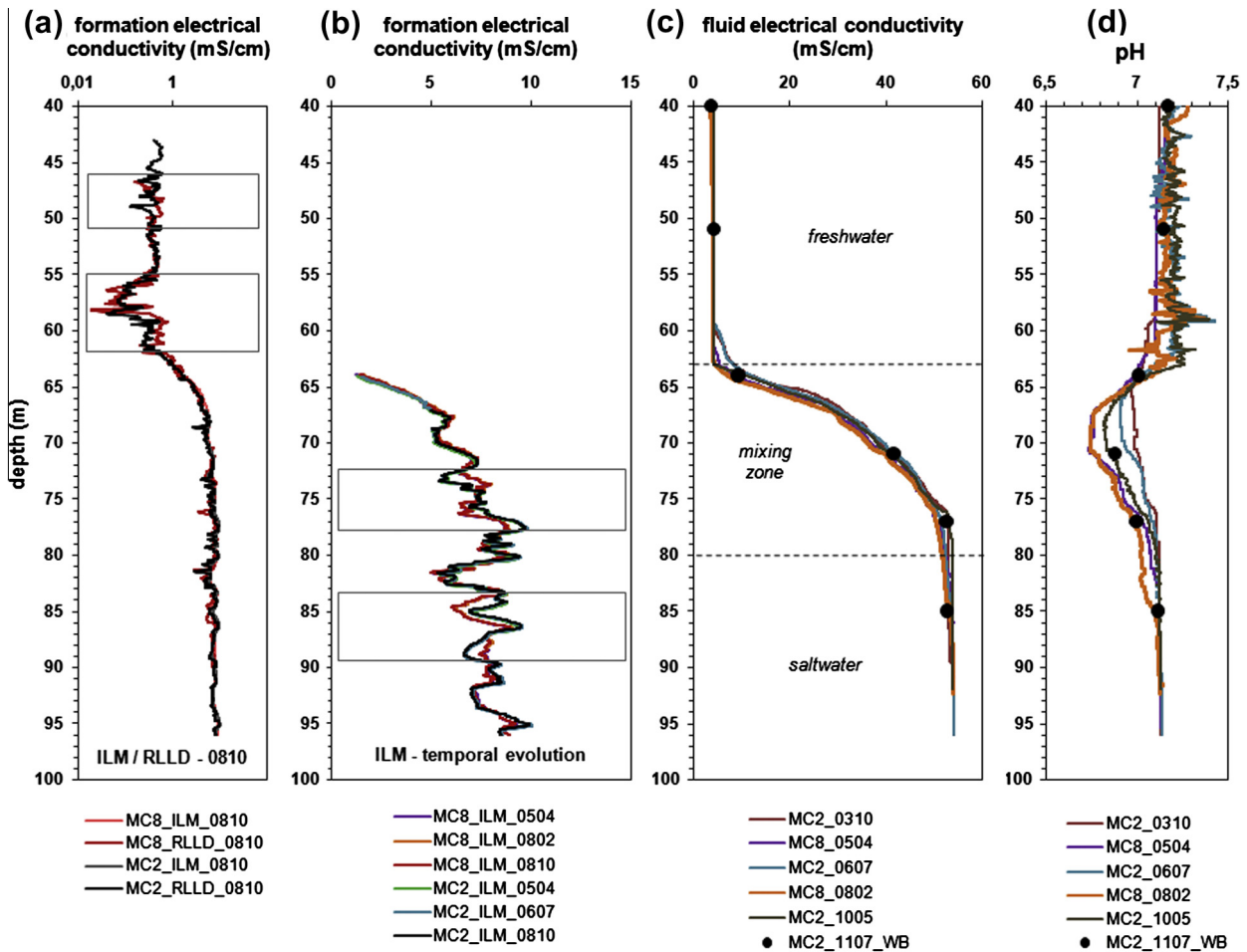


Fig. 2. Downhole geophysical profiles of (a) the electrical conductivity of the formation measured in October 2010 using RLLD and ILM profiles, (b) the evolution of the ILM electrical conductivity of the formation with time, (c) the evolution of the fluid conductivity with time, and (d) the evolution of the pH with time. The 4 numbers in the data name stand for the year and month when the data was recorded, and WB stands for the measurements conducted on the water sampled with the Westbay system (black points).

were available and that the technology is particularly efficient in saline environments, the evolution of the formation conductivity with time was investigated with the ILM logs. The logs of MC2 and MC8 are practically superimposed in the forereef unit (61.7–100 mbs) whereas they show slight deviations in the barrier reef unit (25–61.7 mbs).

Fig. 2b displays ILM logs recorded in borehole MC2 in April 2005, July 2006 and October 2008 and in borehole MC8 in April 2005, February 2008 and October 2008. For each borehole, the profiles are very well superimposed, with no visible variations of the formation conductivity, which is linked to the pore-water conductivity, over the years or seasonally. As shown on the previous graph, the conductivity profiles differ locally from one borehole to another.

Fig. 2c displays the evolution with time of fluid electrical conductivity profiles recorded in MC2 in October 2003, July 2008 and May 2010, and in MC8 in April 2005 and February 2008, together with the electrical conductivity measurements of the waters sampled with the Westbay sampling tool in MC2 (40, 51, 64, 71, 77 and 85 mbs) in July 2011. The corresponding data set for pH is presented in Fig. 2d. The fluid conductivity profiles, which denote the salinity profiles, clearly highlight the saltwater intrusion. Indeed, the data show that the freshwater saturating the barrier reef unit becomes brackish in the forereef unit around 62 mbs where the transition between the freshwater and the

saltwater begins. The water at 80 mbs has salinities similar to seawater. With a freshwater head of 1.5 m, the Ghyben-Herzberg equation estimates the depth of the freshwater–saltwater interface at Ses Sitjoles around 100 mbs, which is deeper than the actual location of the mixing zone. The wide mixing zone depicted by the conductivity profiles is measured in both boreholes (MC2 and MC8) from 2003 to 2010 and is also indicated by the conductivity measurements on the sampled groundwater in 2011, which exactly match the borehole conductivity data. By defining the mixing zone as in Abarca et al. (2007), e.g. the zone where the water has a mixing ratio of saltwater between 25% and 75%, the thickness of the mixing zone at Ses Sitjoles is 7 m, and according to the authors it would correspond to a mean dispersivity of 2.5 m.

Although the conductivity profiles are similar in both boreholes and over years, they do show variations which seem to be seasonal: higher conductivities are recorded in summer and autumn in the mixing zone. The results of the continuous monitoring of the conductivity at 60 mbs (sensor H1) and 70 mbs (sensor H2) in MC8 are presented in Fig. 3. The electrical conductivity of the fluid increases in summer–autumn and decreases in spring. It is noted that the variation is low at 60 mbs (from 4.14 to 4.3 mS/cm) while it is higher at 70 mbs (values from 37.1 to 40.5 mS/cm).

The pH profiles (Fig. 2d) show a noticeable acidification within the mixing zone located around 70 mbs. The change of the pH with

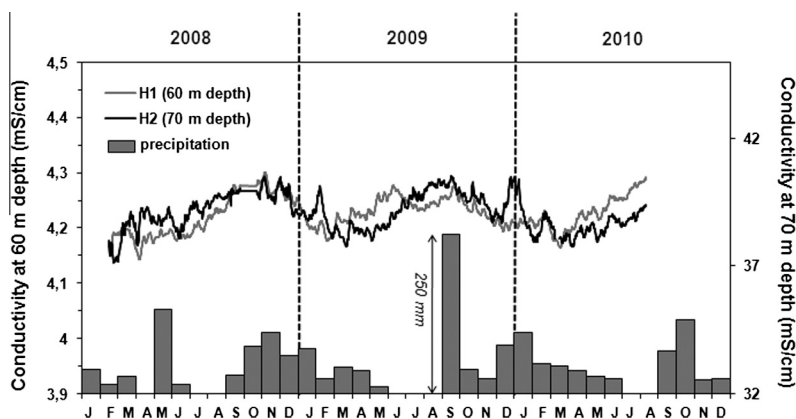


Fig. 3. *In situ* water electrical conductivity monitoring using the Greenspan-Hydraka sensor at 60 mbs (left vertical scale) and 70 mbs in MC8 (right vertical scale), presented together with rain precipitation data.

time shows decreasing pH values with time in borehole MC2 from 2003 to 2011. A careful inspection of the curves indicates a slight shift of the acidification with depth, which is more visible for MC8. However, in contrast to MC2, the results in MC8 do not display any evolution in the acidification at 70 mbs between 2005 and 2008.

3.2. Groundwater characterization within the mixing zone

Groundwater was sampled and analyzed in order to investigate the processes that could be responsible for the acidification reported in the previous paragraph. The concentration of the major elements determined in the water samples are plotted as a function of depth in Fig. 4. The data show that the chemical composition of the waters is unchanged over the period of 6 a in the mixing zone, but some differences are observed below the mixing zone. Yet, it is worth noticing that the waters sampled with the Westbay sampling tool (WB) in the formation show similar concentrations to the ones sampled in the borehole (BH), except again in the saline part around 85 mbs. The data also show that the ion concentrations follow the same trend as the Cl^- concentration with depth, except for Ca.

The saturation indices for calcite and dolomite are displayed as a function of depth in Figs. 5a and b. The groundwater is supersaturated with respect to calcite at 40 mbs and then becomes undersaturated with respect to calcite from 60 to 95 mbs with maximum undersaturation located around 77 mbs. The groundwater is supersaturated with respect to dolomite from 40 to 95 mbs, with maximum supersaturation from 80 to 95 m depth.

These results are now compared to those that would be predicted by conservative mixing. The water end-members used to perform the PHREEQC simulation of the conservative mixing are the freshwater at 40 mbs and the saltwater at 85 mbs in MC2, with regard to the concentrations determined on the waters sampled in July 2011. These concentrations, measured from extracting the water from the formation with the Westbay sampling tool, are assumed to be more representative of the pore-water compared to water sampled within the open borehole and include *in situ* pH and dissolved O_2 measurements. The chemical compositions of these two end-members (40 m and 85 mbs) are given in Table 2. The mean chemical composition of the seawater (SW) is also reported in the table for comparison. The seawater and the saltwater in MC2 at 85 mbs exhibit distinctly different concentrations for the major elements. The seawater, as described in Table 2, in its superficial environment (pH around 8.1–8.2 and pCO_2 equilibrates with

the atmosphere) is noticeably supersaturated with respect to both calcite and dolomite ($\text{SI}_c = 0.71$ and $\text{SI}_d = 2.45$) while the intruded saltwater observed at Ses Sitjoles (located 6 km inland from the coast) is slightly undersaturated with respect to calcite ($\text{SI}_c = -0.06$) and less supersaturated with respect to dolomite ($\text{SI}_d = 0.64$) (see Table 2).

The difference between the Ca and Mg concentrations in the analyzed water and those predicted by a conservative mixing of the freshwater at 40 mbs and the saltwater at 85 mbs (ΔCa and ΔMg , respectively) are plotted as a function of depth in Fig. 5c and d. The Ca and Mg concentrations in freshwater samples from 40 to 62 mbs are similar to those for conservative mixing, whereas the Ca and Mg concentrations measured from 62 to 95 mbs differ from the theoretical mixing curve. The maximum discrepancy for the Ca is at 70 mbs, which does not match the maximum calcite undersaturation located at around 77 mbs (Fig. 5a). It is noted that the Ca concentration and, therefore, its deviation from the mixing curve is stable in time (from 2005 to 2011) and remarkably similar in MC2 and MC8. The excess of Mg is also measured in both boreholes from 75 to 95 mbs and also appears stable in time: ΔMg is about 5 mmol/L for all these samples. The results for Ca and Mg concentrations and the calcite and dolomite saturation index are presented as a function of the mixing ratio in Fig. 6. The figure also shows the evolution of pH and pCO_2 with the mixing ratio. In each case the data are compared to the results that would give conservative mixing (full line). The theoretical mixing of the freshwater and saltwater indicates a maximum undersaturation of water with respect to calcite for mixing ratios ranging from 30% to 60%, which corresponds to a depth around 65 mbs, whereas greater undersaturation is actually reached for a mixing ratio of 85% at Ses Sitjoles (corresponding to 77 mbs). The dolomite saturation index for conservative mixing also does not match the saturation index calculated from the field data. However, in both cases, the maximum supersaturation with respect to dolomite is reached for a mixing ratio higher than 90% and the maximum saturation index values are around 0.6. As far as pH and log pCO_2 are concerned, the measured data show lower values of pH and higher values of pCO_2 than the theoretical calculated ones. The maximum acidification, which corresponds approximately to the maximum values of pCO_2 and Ca concentration, is obtained for a mixing ratio of $64 \pm 3\%$ of saltwater (corresponding to approximately 70 m depth).

Analyses of the total organic C (TOC) and dissolved O_2 were also conducted on groundwater sampled in July 2011 with the Westbay system. The data are presented in Fig. 7 versus depth, together

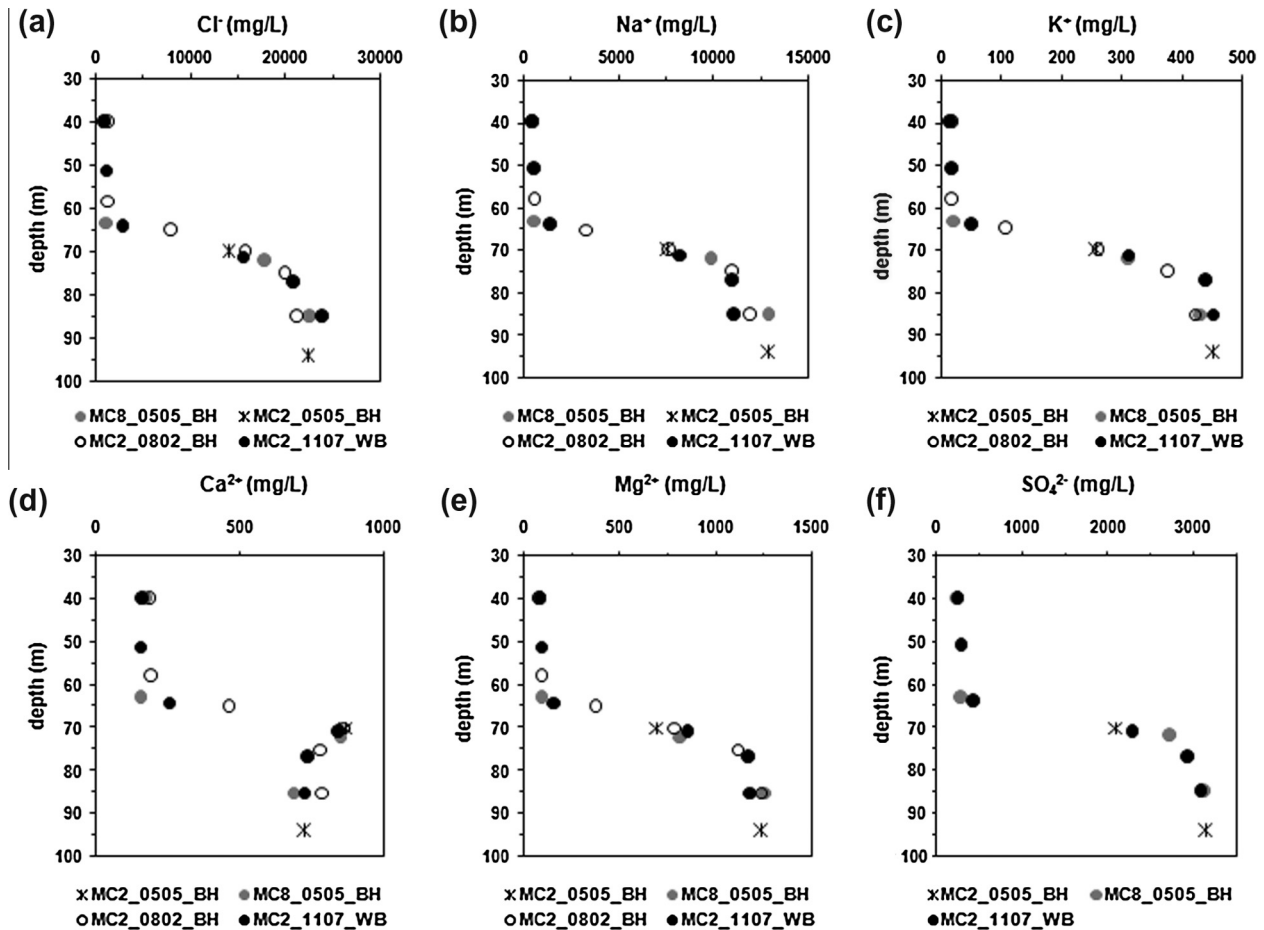


Fig. 4. Evolution of the concentrations of Cl⁻, Na, K, Ca, Mg and SO₄²⁻ with depth, determined in MC2 and MC8 in May 2005 (MC2_0505_BH and MC8_0505_BH, where BH denotes waters sampled in the borehole with a bailer), in MC2 in February 2008 (MC2_0802_BH) and in July 2011 (MC2_1107_WB, where WB denotes waters sampled using the Westbay equipment).

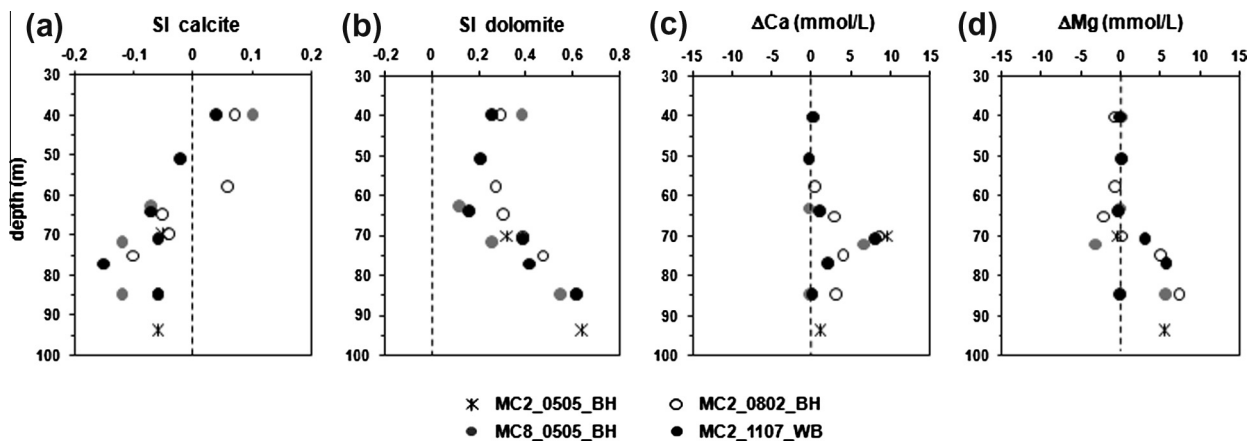


Fig. 5. Saturation index (SI) of the analyzed waters with respect to calcite (a) and dolomite (b) calculated with PHREEQC and the difference between the Ca and Mg concentrations in the actual water and those assuming a simple mixing of the freshwater at 40 mbs and the saltwater at 85 mbs: ΔCa (c) and ΔMg (d).

with the pH and log(pCO₂). The results show a maximum concentration of dissolved organic C and a depletion of O₂ in the vicinity of 70 mbs, coinciding with the lowest pH values and highest pCO₂ content reported above.

3.3. Reservoir rock properties

Porosity and permeability were measured on plugs sampled in the core extracted from borehole MC2. The porosity values

Table 2

Chemical composition of the freshwater at 40 m depth and the saltwater at 85 m depth in MC2 (July 2011, Westbay samples) and chemical composition of the Mediterranean seawater (sampled at the coast 6 km from the experimental site).

	Na ⁺	Cl ⁻	Ca ²⁺	Mg ²⁺	K ⁺	SO ₄ ²⁻	HCO ₃ ⁻	pH	T (°C)	SI _c	SI _d	Log(pCO ₂)
	mmol/L											
40 m	21.59	27.08	4.14	3.45	0.42	2.68	4.31	7.17	23.87	0.04	0.26	-1.83
85 m	486.1	678.4	18.01	48.68	11.57	32.00	2.37	7.12	24.86	-0.06	0.64	-2.21
SW	516.7	610.7	11.28	58.79	12.16	29.71	2.59	8.17	–	0.71	2.45	-3.30

of the rock samples from the mixing zone are around 0.45, except for two samples located at 74 and 77 mbs, which exhibit lower values of porosity around 0.20. The corresponding permeability data are scattered, with values ranging from 10 mD ($9.87 \times 10^{-15} \text{ m}^2$) to 1400 mD ($1.48 \times 10^{-12} \text{ m}^2$) and a mean value of 150 mD ($1.48 \times 10^{-13} \text{ m}^2$). The highest values of permeability are found for the samples at 74 and 77 mbs, which has the smallest porosity values. These two samples clearly stand out from the data set.

Optical borehole-wall images were used to visualize the reservoir structure and especially locate specific dissolution features in the mixing zone. The images obtained in MC2 and MC8 from 64 to 94 mbs are shown in Fig. 8. The rock structure clearly shows an enhancement of porosity from 72 to 85 mbs in both boreholes, with more porosity development in MC8. Large dissolution vugs of up to 50 cm are observed in MC2 at 79.5 mbs, which corresponds

to the zone where the water has been measured as most undersaturated with respect to calcite. Note that this depth is about 2 m below the depth for which the maximum undersaturation was predicted. Around 70 mbs, which corresponds to the zone characterized by lower pH and dissolved O₂ values and higher CO₂ and organic content as well as Ca concentration, the borehole-wall images do not show particular porosity features in MC2, whereas many vugs are visible in MC8.

4. Discussion

Repeated measurements of the electrical conductivity profile in the boreholes with time did not show any changing trend of saltwater intrusion from 2003 to 2011. The monitoring of the water chemical composition also suggests that the

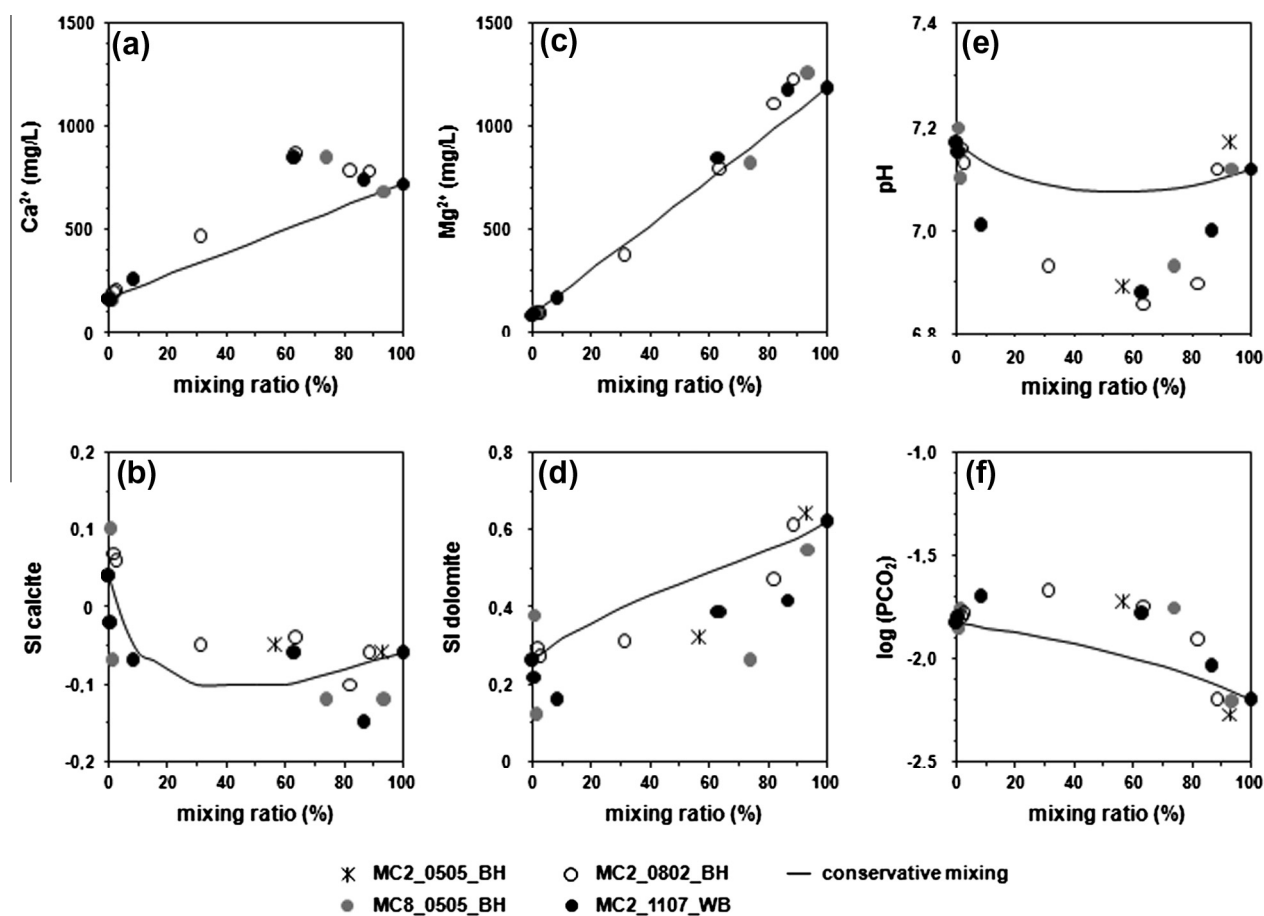


Fig. 6. Calcium and Mg concentration (graphs a and c, respectively), calcite and dolomite saturation index (graphs b and d, respectively), pH (graph e) and log(pCO₂) (graph f) plotted as a function of the mixing ratio (% of saltwater in the mixing), and compared with the theoretical conservative mixing of the two end-member waters (40 m depth and 85 m depth).

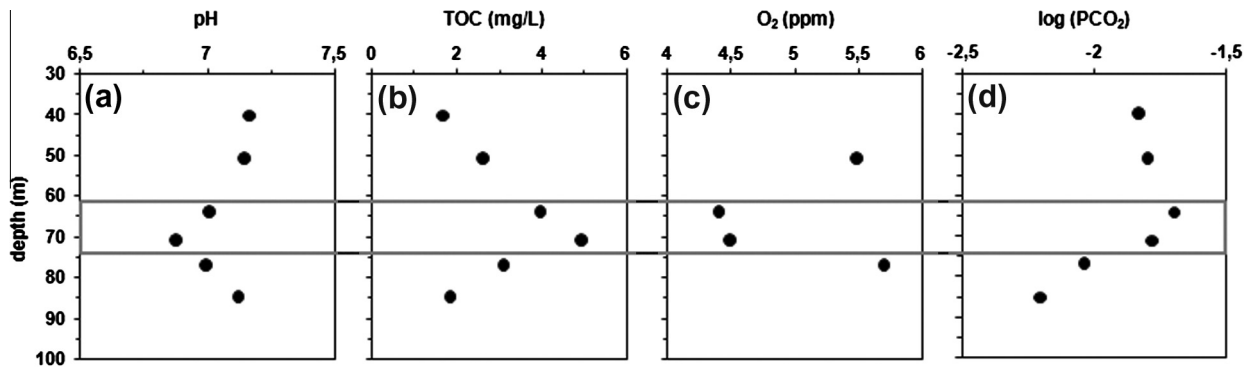


Fig. 7. pH (a), total organic C (b), dissolved O_2 (c) conducted, and $\log(pCO_2)$ (d) obtained from the determined chemical composition of the water sampled with the Westbay System in MC2 in July 2011.

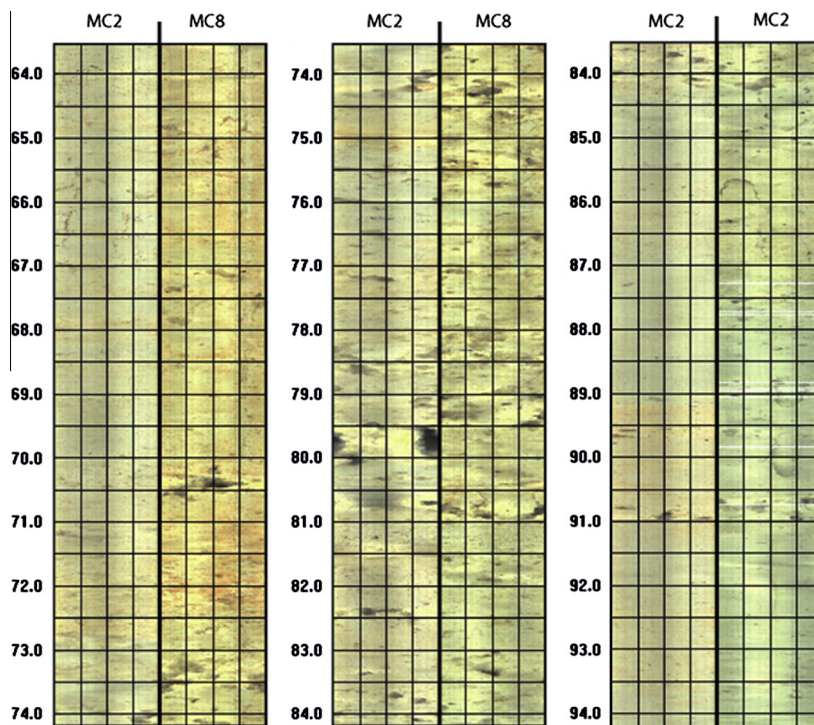


Fig. 8. Optical borehole wall image recorded in MC2 in November 2003 and in MC8 in July 2004.

freshwater–saltwater mixing zone has not evolved during that short period of time. The mixing zone characterized by the conductivity and ion concentrations appears to be much wider than usual: indeed, sharp fronts are commonly observed on salinity profiles (from electrical conductivity profiles mostly) and sampled pore water salinity data and predicted from models, as reviewed by Abarca et al. (2007). These authors proposed a relationship between the width of the mixing zone and the dispersivity, however, in the case of the mixing zone encountered at the Ses Sitjoles site it would correspond to a mean dispersivity of 2.5 m, whereas Le Borgne and Gouze (2008) determined a value on the order of a few centimeters from tracer tests at depth 90 in borehole MC2. Also, the depth of the freshwater/saltwater interface could not be explained using the Ghyben-Herzberg approximation, but a more accurate estimation of the location of the mixing zone using for instance the model proposed by Abarca et al. (2007) requires hydrodynamic data, such as the inland freshwater flux, the seaside saltwater flux and the hydraulic conductivity of the reservoir. Heat pulse flowmeter measurements and spontaneous potential profiles

recorded in MC8 by Pezard et al. (2009) demonstrated the existence of vertical and horizontal flows in the karstified reef barrier unit, whereas no flow was detected in the foreereef unit. However, these studies did not provide quantitative flow rate data, necessary to model the inland penetration of the saltwater and explain the location and shape of the mixing zone.

High-frequency monitoring of the groundwater conductivity revealed seasonal variations of conductivity linked to the rainfall cycle and probably to freshwater withdrawal. Accurate details on the groundwater withdrawals in the area for agricultural and touristic purpose would be needed to further investigate the impact of water resource utilization on saltwater intrusion. During the time of the present study it did not affect the overall location of the mixing zone, however, within the last 50 a, the progression of the seawater inland, associated with the upwelling of the saltwater body is clearly reported by local farmers who progressively find saltwater at depths where the water was fresh previously.

From the chemical characterization of the groundwater in the mixing zone, three zones showing distinctly different features

can be determined: i) the zone around 77 mbs where maximum calcite undersaturation is found, ii) the zone from 84 to 90 mbs where supersaturation with respect to dolomite is highest and iii) the center of the mixing zone around 70 mbs, which is characterized by a lower pH, higher $p\text{CO}_2$ and higher Ca concentration than predicted by conservative mixing.

The maximum calcite undersaturation occurring on the saltwater side of the mixing zone (around 77 mbs) cannot be explained by conservative mixing, which predicts maximum undersaturation for a lower mixing ratio and does not match the maximum Ca concentrations measured around 70 mbs. The petrophysical measurements conducted on the MC2 plugs do not show higher porosity values where the maximum undersaturation is calculated, but they show much higher permeability values (from 75 to 80 mbs). Dissolution features can be observed on the borehole wall images, suggesting that the geochemistry of the water at these depths results in porosity development due to calcite dissolution. However, the major dissolution features are located slightly deeper than the presently observed maximum undersaturation, which suggests an upward motion of the saltwater body. In addition, the dissolution events have probably increased the pre-existing small-scale heterogeneity of the reservoir, resulting in differences in the pore structure between boreholes MC2 and MC8, as indicated on the images (Fig. 8) and also on the formation conductivity profiles (Fig. 2b).

Dolomite is found in the higher conductivity part of the aquifer (85–90 mbs) where the groundwater supersaturated with respect to dolomite. In this zone, $SI_{\text{calcite}} < 0$ and $SI_{\text{dolomite}} > 0$ and the $[\text{Mg}]/[\text{Ca}]$ ratio is larger than unity, which are reported as ideal conditions for dolomitization by Wigley and Plummer (1976) and Margaritz et al. (1980). However, water samples from 75 to 95 mbs indicate an excess in Mg, which would be more in favor of dolomite dissolution than dolomitization. The origin of these Mg concentrations is not yet understood. In particular, it contradicts the above statements and previous thin section analysis of MC2 borehole core.

At around 70 mbs, the Ca concentration is much higher than expected from conservative mixing and does not correspond to the maximum undersaturation with respect to calcite calculated from the groundwater chemical analysis. The ubiquitous pH acidification at these depths (Fig. 2d and e) and higher CO_2 content (Fig. 6f) cannot be explained by mixing of freshwater and saltwater only. This acidification is accompanied by an increase in organic C and a decrease in dissolved O_2 (Fig. 7). Therefore, it is inferred that the presence of microorganisms around 70 mbs, which consume O_2 and release CO_2 , might be responsible for the acidification and, as the result, for the induced calcite dissolution, as conjectured by Smart et al. (1988), Whitaker and Smart (1997) and Baceta et al. (2001). A better characterization of the on-going biogeochemical processes within the mixing zone would require the quantification and identification of the microorganisms present in the mixing zone.

The reported difference in the pH evolution (Fig. 2d) between MC8, where the acidification has not evolved since the drilling of the borehole, and MC2, where the acidification was minor just after drilling and then increased continuously from 2003 could be explained by the fact that microorganisms were already present in MC8 by the time of drilling, whereas they were not present in MC2 and developed after the drilling. The main difference between these two boreholes in the center of the mixing zone (50% saltwater–50% freshwater) at depths around 70 mbs is the presence of highly connected porosity and so highest permeability in MC8 (Fig. 8). It is conjectured that the large permeability in MC8 triggers significant renewal of the water and, therefore, promotes biomass colonization by maintaining favorable conditions. Conversely, it is supposed that borehole MC2 was initially free of biomass because

of the presence of more confined water (lower permeability and vertical connectivity than in MC8). However, the presence of the borehole might have boosted the water renewal capacity in the mixing zone due to by-passing the different water levels, allowing progressive colonization of the reservoir by biomass in the vicinity of the well. As a generalization from these observations, it is proposed that (i) the development of perennial biomass is correlated to permeability and vertical connectivity at the meter-scale as is the microbiologically-enhanced dissolution and (ii) the mechanism could be self-activated because the microbiological activity induces calcite dissolution and, therefore, tends to increase permeability.

5. Conclusions

This study reports long-term (9 a) high resolution multi-parameter *in situ* monitoring of a mixing zone, allowing an unmatched characterization of a saltwater intrusion. Combining the electrical formation and fluid conductivity logs, pH and ion-concentration measurements, it can be inferred that calcite dissolution is occurring in the mixing zone at the Ses Sitjoles site. However, nothing can be concluded at this stage regarding dolomite. Yet, the chemical composition of the water is significantly different from that predicted by fluid–rock interaction models and hydrodynamic mixing. From the combined analysis of the time-resolved pH profile, the porosity and the organic content, a model is proposed in which calcite dissolution is enhanced in the center of the mixing zone (50% freshwater/50% seawater) by microbiological activity that decreases the pH and significantly influences the local geochemistry. The development of biomass seems to concentrate in zones where fluid mixing is active, i.e. where porosity and permeability are sufficiently high. This suggests that microbiological activity is probably disseminated in clusters associated with high flow rate. Finally it is reported that the main dissolution features identified from core analysis and borehole geophysical measurements appear to be slightly deeper (1–3 m) than the measured maximum undersaturation, indicating an upward motion of the mixing zone that can be coherently linked with the progression inland of the seawater intrusion. It is also noted that the mixing zone is significantly thicker than is usually observed in similar environments and predicted by the hydrodynamical models, but the origin of the width of the mixing zone is still an open question.

Acknowledgments

We wish to acknowledge TOTAL and the CNRS for their financial support to conduct this field study. We also thank the Environmental Ministry of the Government of the Balearic Islands, in the persons of Concha Gonzalez and Alfredo Baron, for their encouragement and support for the development of the experimental site at Ses Sitjoles.

References

- Abarca, E., Carrera, J., Sanchez-Vila, X., Dentz, M., 2007. Anisotropic dispersive Henry problem. *Adv. Water Resour.* 30, 913–926.
- Appelo, C.A.J., Postma, D., 1993. *Geochemistry Groundwater and Pollution*. A. A. Balkema Publishers, Rotterdam.
- Arfib, B., de Marsily, G., 2004. Modeling the salinity of an inland coastal brakishkarstic spring with a conduit-matrix model. *Water Resour. Res.* 40, W11, 506.
- Baceta, J.I., Wright, P., Pujalte, V., 2001. Palaeo-mixing zone karst features from Palaeocene carbonates of north Spain: criteria for recognizing a potentially widespread but rarely documented diagenetic system. *Sed. Geol.* 139, 205–216.
- Bear, J., Cheng, A.H.D., Sorek, S., Ouazar, D., Herrera, I., 1999. *Seawater Intrusion in Coastal Aquifers – Concepts, Methods and Practices*. Kluwer Academic Publishers, Dordrecht, The Netherlands.
- Black, W.H., Smith, H.R., Patton, F.D., 1986. Multiple-level groundwater monitoring with the MP System. In: *Proc. Surface and Borehole Geophysical Methods and*

- Groundwater Instrumentation Conference and Exposition, Denver, CO, October 15–17, pp. 41–61.
- Cooper Jr., H.H., 1964. A Hypothesis concerning the Dynamic Balance of Fresh Water and Salt Water in a Coastal Aquifer. U.S. Geol. Surv. Water-Supply Paper 1613-C.
- Deya Tortella, B., Tirado, D., 2011. Hotel water consumption at a seasonal mass tourist destination. The case of the island of Mallorca. *J. Environ. Manage.* 92, 2568–2579.
- Esteban, M., 1979. Significance of the upper Miocene reefs in the western Mediterranean. *Paleogeogr. Palaeoclimatol. Palaeoecol.* 29, 169–188.
- Garing, C., 2011. Caractérisation géophysique et géochimique des interactions fluide-roche à l'interface eau douce-eau salée : cas des carbonates récifaux de Majorque. Ph.D. Thesis. Univ. Montpellier 2, Montpellier, France.
- Ghyben, B.W., 1889. Nota in verband met de voorgenomen putboring nabij Amsterdam. In: *The Hague. K. Inst. Ing. Tydschrift*, pp. 8–22.
- Gonzales, L.A., RuizH, M., 1991. Diagenesis of middle tertiary carbonates in the Toa Baja well, Puerto Rico. *Geophys. Res. Lett.* 18, 513–516.
- Hanshaw, B.B., Back, W., 1980. Chemical mass-wasting of the northern Yucatan Peninsula by groundwater dissolution. *Geology* 8, 222–224.
- Hebert, V., 2011. Analyses multi-échelles de la structure d'un réservoir carbonaté littoral: exemple de la plateforme de Llucmajor (Majorque, Espagne). Ph.D. Thesis. Univ. Montpellier 2, Montpellier, France.
- Henry, H.R., 1964. Effects of Dispersion on Salt Encroachment in Coastal Aquifers. U.S. Geol. Surv. Water-Supply Paper 1613-C.
- Herzberg, A., 1901. Die Wasserversorgung einiger Nordseebäder. In: *J. Gasbeleuchtung und Wasserversorgung*, 44, Munich, Germany, 815–819/842–844.
- Jaeggi, D., 2006. Multiscalar Porosity Structure of a Miocene Reefal Carbonate Complex. Ph.D. Thesis. ETH, Zurich, Switzerland.
- Jones, B.F., Vengosh, A., Rosenthal, E., Yechieli, Y., 1999. Chapter 3: geochemical investigations. In: Bear, J., Cheng, A.H.D., Sorek, S., Ouazar, D., Herrera, I. (Eds.), *Seawater Intrusion in Coastal Aquifers – Concepts*. Kluwer Academic Publishers, Dordrecht, The Netherlands, pp. 1–72.
- Jones, S.C., 1972. A rapid unsteady state Klinkenberg permeameter. *Soc. Petrol. Eng. J.* 12, 383–397.
- Kent, M., Newnham, R., Essex, S., 2002. Tourism and sustainable water supply in Mallorca: a geographical analysis. *Appl. Geogr.* 22, 351–374.
- Klinkenberg, L.J., 1941. The permeability of porous media to liquids and gases. In: *API Drilling and Production Practice*, API 11th Mid-Year Meeting, Tulsa, OK (May 1941), pp. 200–213.
- Le Borgne, T., Guze, P., 2008. Non-Fickian dispersion in porous media: 2. Model validation from measurements at different scales. *Water Resour. Res.* 44, W06427. <http://dx.doi.org/10.1029/2007WR006279>.
- Llomas, M.R., Custodio, E., 2003. Intensive Use of Groundwater: Challenges and Opportunities. Balkema Publishers, The Netherlands.
- Maliva, R.G., Missimer, T.M., Walker, C.W., Owsina, E.S., Dickson, J.A.D., Fallick, A.E., 2001. Carbonate diagenesis in a high transmissivity coastal aquifer, Biscayne aquifer, southeastern Florida, USA. *Sed. Geol.* 143, 287–301.
- Margaritz, M., Golgenberg, L., Kafri, U., Arad, A., 1980. Dolomite formation in the seawater–freshwater interface. *Nature* 287, 622–624.
- Maria-Sube, Y., 2008. Structure et hétérogénéité d'une plateforme récifale Miocène (Majorque), implication pour les intrusions d'eau salée en zone côtière. Ph.D. Thesis. Univ. Montpellier 2, Montpellier, France.
- Melim, L.A., Westphal, H., Swart, P.K., Eberli, G.P., Munnecke, A., 2002. Questioning carbonate diagenetic paradigms: evidence from the Neogene of the Bahamas. *Mar. Geol.* 185, 27–53.
- Ng, K., Jones, B., 1995. Hydrogeochemistry of Grand Cayman, British West Indies: implications for carbonate diagenetic studies. *J. Hydrol.* 164, 193–216.
- Parkhurst, D.L., Appelo, C.A.J., 1999. User's Guide to PHREEQC (Version 2) – A Computer Program for Speciation, Batch-reaction, One-dimensional Transport, and Inverse Geochemical Calculations. U.S. Geol. Surv. Water-Resour. Invest. Rep. 99-4259.
- Pezard, P.A., Gautier, S., Le Borgne, T., Legros, B., Deltombe, J.L., 2009. MuSET: a multiparameter and high precision sensor for downhole spontaneous electrical potential measurements. *C. R. Geosci.* 341, 957–964.
- Plummer, L.N., 1975. Mixing of sea water with calcium carbonate ground water. *Geol. Soc. Am. Mem.* 142, 219–236.
- Pomar, L., Ward, W.C., 1999. Reservoir-scale heterogeneity in depositional packages and diagenetic patterns on a reef-rimmed platform, Upper Miocene, Mallorca, Spain. *Am. Assoc. Petrol. Geol. Bull.* 83, 1759–1773.
- Pomar, L., Ward, W.C., Green, D.G., 1996. Upper Miocene reef complex of the Llucmajor area, Mallorca, Spain. *SEPM Concepts Sedimentol. Paleontol.* 5, 191–225.
- Price, R.M., Herman, J.S., 1991. Geochemical investigation of salt-water intrusion into a coastal carbonate aquifer: Mallorca, Spain. *Geol. Soc. Am. Bull.* 103, 1270–1279.
- Pulido-Leboeuf, P., 2004. Seawater intrusion and associated processes in a small coastal complex aquifer (Castell de Ferro, Spain). *Appl. Geochem.* 19, 1517–1527.
- Rezaei, M.R., Sanz, E., Raeisi, E., Ayora, C., Vazquez-Suné, E., Carrera, J., 2005. Reactive transport modeling of calcite dissolution in the fresh–salt water mixing zone. *J. Hydrol.* 311, 282–298.
- Romanov, D., Dreybrodt, W., 2006. Evolution of porosity in the saltwater–freshwater mixing zone of coastal carbonate aquifers: an alternative modelling approach. *J. Hydrol.* 329, 661–673.
- Runnels, D.D., 1969. Diagenesis, chemical sediments, and the mixing of natural waters. *J. Sed. Petrol.* 39, 1188–1201.
- Sandford, W.E., Konikow, L.F., 1989a. Porosity development in coastal carbonate aquifers. *Geology* 17, 249–252.
- Sandford, W.E., Konikow, L.F., 1989b. Simulation of calcite dissolution and porosity changes in saltwater mixing zones in coastal aquifers. *Water Resour. Res.* 25, 655–667.
- Sanz, E., Ayora, C., Carrera, J., 2011. Calcite dissolution by mixing waters: geochemical modeling and flow-through experiments. *Geol. Acta* 9, 67–77.
- Schlumberger, 1972. *Log interpretation, Vol. I: Principles*. New York, Schlumberger Limited, 113 p.
- Schlumberger, 1974. *Log interpretation, Vol. II: Applications*. New York, Schlumberger Limited, 116 p.
- Singurindy, O., Berkowitz, B., Lowell, R.P., 2004. Carbonate dissolution and precipitation in coastal environments: laboratory analysis and theoretical consideration. *Water Resour. Res.* 40, W04401. <http://dx.doi.org/10.1029/2003WR002651>.
- Smart, P.L., Dawans, J.M., Whitaker, F., 1988. Carbonate dissolution in a modern mixing zone. *Nature* 335, 811–813.
- Stoessel, R.K., Ward, W.C., Ford, B.H., Schuffert, J.D., 1989. Water chemistry and CaCO₃ dissolution in the saline part of an open-flow mixing zone, coastal Yucatan Peninsula, Mexico. *Geol. Soc. Am. Bull.* 101, 159–169.
- Vengosh, A., 2003. Salinization and saline environments. In: *Sherrwood Lollar, B. (Ed.), Environmental Geochemistry*. Holland, H.D., Turekian, K.T. (Exec. Eds.), *Treatise on Geochemistry* 9. Elsevier Science.
- Whitaker, F.F., Smart, P., 1997. Groundwater circulation and geochemistry of a karstified bank-marginal fracture system, south Andros Island, Bahamas. *J. Hydrol.* 197, 293–315.
- Wicks, C.M., Herman, J.S., 1996. Regional hydrogeochemistry of a modern coastal mixing zone. *Water Resour. Res.* 32, 401–407.
- Wigley, T.M.L., Plummer, L.N., 1976. Mixing of carbonate waters. *Geochim. Cosmochim. Acta* 40, 989–995.